Preprints, 4th IFAC Conference on
Advances in Proportional-Integral-Derivative Control
Almería, Spain | June 12-14, 2024

An IMC decentralized PID controller retuning method based on frequency domain data.

Egydio T. G. Ramos * **George Acioli Júnior** **
Péricles R. Barros **

* *Post-Graduate Program in Electral Engineering, Electrical Engineering Department, Federal University of Campina Grande, Brazil (e-mail: egydio.ramos@ee.ufcg.edu.br).*
** *Electrical Engineering Department, Federal University of Campina Grande, Brazil (e-mail: [georgeacioli, prbarros]@dee.ufcg.edu.br).*

Abstract: In this work, a method is proposed for retuning decentralized proportional-integral-derivative controllers. It consists in applying the internal model control approach in order to fit the closed-loop frequency response to that of a desired reference model. Then, an optimization problem is solved to adjust the increments on the controller parameters in order to meet the closed-loop requirements. To guarantee stability and robustness, linear margin constraints are applied to each loop, using the concept of effective loop transfer functions to take the coupling into account. The procedure is validated through simulations studies, by comparing it with other decentralized and centralized tuning methods.

Keywords: Decentralized control, PID control, internal model control.

1. INTRODUCTION

Many industrial processes are multi-input and multi-output (MIMO). The coupling between loops is a major issue for achieve stability and performance requirements during the control design of this process. In literature, several control strategies are proposed, to tune controllers with centralized or decentralized structures. The simplest consists in the decentralized proportional-integral (PI) or proportional-integral-derivative (PID) structures, which are easy to implement and leads to good solutions in most applications (Nisi et al., 2019).

To address the issues caused by loops interactions in decentralized control, different approaches can be taken. One consists in use MIMO stability criteria during design, such as the Nyquist criterion or Gershgorin bands. The latter is used in Euzébio et al. (2020), where it is presented the design of decentralized PID controllers, by solving a linear programming problem. The main disadvantage was that this approach is too conservative, being applicable only to diagonal dominant process.

Other approach is to divide the MIMO system into several single-input and single-output (SISO) subsystems, and take the loop interactions into account by using the concept of effective transfer function (ETF). In Silva and Barros (2020) and Garrido et al. (2022), the ETF and the effective loop transfer function (ELTF) are applied, respectively, to design decentralized and centralized controllers. The stability and robustness of each subsystem is assured by applying constraints in the Nyquist diagrams, using a method proposed by Karimi et al. (2007).

Methods based on internal model control (IMC) are also used to specify the closed-loop desired responses. This approach is applied in Jeng and Lee (2023), where a diagonal reference model is defined to specify the desired performance. Then the specifications of the off-diagonal terms are chosen in order to make the controller matrix diagonal. Frequency domain data is used to formulate a least square problem to approximate the controller desired frequency response by a decentralized PID structure.

In Gao et al. (2017), it is said that around 60% of industrial controllers suffer from certain types of malfunctions. The main causes of this malfunctions are the poorly tuned controller parameters and the changes in the plant structure. Then, it is proposed a data-driven method for performance assessment and retuning of PID controllers.

In Silva Moreira et al. (2021), an internal model control (IMC) returning method for PID controllers is presented. It uses only process frequency domain data, and is restricted to SISO systems. The method is extended to square MIMO processes in Aguiar et al. (2021). The resulting controllers are centralized.

In this paper, a method for retuning decentralized PID controllers is proposed. Given the initial controller gains and the frequency response of the process, the aim is to obtain the gains increments based on a closed-loop desired specification. To ensure stability and robustness, margin constraints are imposed to each loop, by taking into account the interactions using the ETF approach. Then, a convex optimization problem is stated to solve the problem with the constraints.

⋆ This work was supported by CAPES, Brazil.

This paper is organized as follows. In Section 2 the control problem is defined. The proposed method is presented in Section 3. Simulation studies are shown in Section 4. Conclusions are discussed in Section 5.

2. PROBLEM STATEMENT

Consider the closed-loop system block diagram presented in Fig. 1. It is a $n \times n$ MIMO process where:

$$\mathbf{G}(s) = \begin{bmatrix} G_{11}(s) & G_{12}(s) & \cdots & G_{1n}(s) \\ G_{21}(s) & G_{22}(s) & \cdots & G_{2n}(s) \\ \vdots & \vdots & \ddots & \vdots \\ G_{n1}(s) & G_{n2}(s) & \cdots & G_{nn}(s) \end{bmatrix}. \quad (1)$$

Here, $G_{ij}(s)$ is the transfer function between jth input and ith output. The system is in closed-loop with an initial decentralized controller:

$$\mathbf{C}^0(s) = \text{diag}\left[C_1^0(s), C_2^0(s), \cdots, C_n^0(s)\right]. \quad (2)$$

The jth loop term of the controller has the following parallel PID form:

$$C_j^0(s) = k_{P_j}^0 + \frac{k_{I_j}^0}{s} + \frac{k_{D_j}^0 s}{T_{fj}s + 1}, \quad (3)$$

where $k_{P_j}^0$, $k_{I_j}^0$ and $k_{D_j}^0$ are the jth loop proportional, integral and derivative gains, respectively. T_{fj} is the derivative filter time constant, which is assumed to be known.

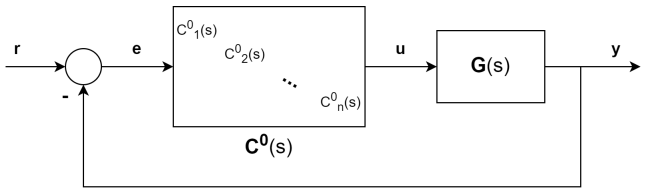

Fig. 1. Decentralized control system block diagram.

For this system, the complementary sensitivity matrix is defined as:

$$\mathbf{T}^0(s) = \left(\mathbf{I} + \mathbf{G}(s)\mathbf{C}^0(s)\right)^{-1} \mathbf{G}(s)\mathbf{C}^0(s). \quad (4)$$

Given $\mathbf{T}^0(s)$ and $\mathbf{C}^0(s)$, the problem consists in obtain a new PID decentralized controller, named $\mathbf{C}(s)$, such that the new closed-loop transfer matrix, $\mathbf{T}(s)$, approaches a specified dynamics given by $\mathbf{T_r}(s)$.

Assuming that the elements of $\mathbf{G}(s)$ have no zeros on RHP, then:

$$\mathbf{T_r}(s) = \text{diag}\left[\frac{e^{-L_{11}s}}{\tau_1 s + 1}, \cdots, \frac{e^{-L_{nn}s}}{\tau_n s + 1}\right], \quad (5)$$

where τ_j is the specified time constant for jth loop and L_{jj} is the time delay of $G_{jj}(s)$.

3. CONTROLLER RETUNING METHOD

In this section, the proposed procedure to retuning decentralized PID controllers will be presented. An optimization problem will be formulated to approximate the frequency response between the complementary sensitivity matrix and the desired specification.

To guarantee closed-loop stability and robustness, constraints on the Nyquist diagram are added to the optimization problem. This is done by using the effective transfer function (ETF) to account for loop interactions, such that SISO stability margins limits can be imposed for each loop.

3.1 Controller design

Given the initial controller ($\mathbf{C}^0(s)$), the designed controller can be expressed as:

$$\mathbf{C}(s) = \mathbf{C}^0(s) + \mathbf{C}^\Delta(s), \quad (6)$$

where $\mathbf{C}^\Delta(s)$ is the increment transfer matrix.

The problem of PID IMC controller retuning was first proposed in Silva Moreira et al. (2021). In Aguiar et al. (2021), the problem was extended to redesign centralized controllers. Here, the case of PID decentralized control is treated.

Lemma 1. The increments $\mathbf{C}^\Delta(s)$ in order to meet the specification $\mathbf{T_r}(s)$ are given by:

$$\mathbf{C}^\Delta(s) = \mathbf{C}^0(s)\left(\mathbf{T}^0(s)\right)^{-1}\left(\mathbf{T}_r(s) - \mathbf{T}^0(s)\right)\left(\mathbf{S}_r(s)\right)^{-1}. \quad (7)$$

Proof. Defining the following sensitivity functions:

$$\begin{aligned} \mathbf{S}^0(s) &= \mathbf{I} - \mathbf{T}^0(s) = \left(\mathbf{I} + \mathbf{G}(s)\mathbf{C}^0(s)\right)^{-1}, \\ \mathbf{S}(s) &= \mathbf{I} - \mathbf{T}(s) = \left(\mathbf{I} + \mathbf{G}(s)\mathbf{C}(s)\right)^{-1}, \text{ and} \\ \mathbf{S_r}(s) &= \mathbf{I} - \mathbf{T_r}(s). \end{aligned} \quad (8)$$

Then:

$$\begin{aligned} &\mathbf{S}^0(s)\left(\mathbf{S}(s)\right)^{-1}\mathbf{S}_r(s) = \\ &= \left(\mathbf{I} + \mathbf{G}(s)\mathbf{C}^0(s)\right)^{-1}\left(\mathbf{I} + \mathbf{G}(s)\mathbf{C}(s)\right)\mathbf{S}_r(s). \end{aligned} \quad (9)$$

Ideally, $\mathbf{S}(s) = \mathbf{S_r}(s)$, which leads to:

$$\mathbf{S}^0(s) = \left(\mathbf{I} + \mathbf{G}(s)\mathbf{C}^0(s)\right)^{-1}\left(\mathbf{I} + \mathbf{G}(s)\mathbf{C}(s)\right)\mathbf{S}_r(s). \quad (10)$$

This equation can be rewritten, using (6) and then (4), as:

$$\mathbf{S}^0(s) = \left[\mathbf{I} + \mathbf{T}^0(s)\left(\mathbf{C}^0(s)\right)^{-1}\mathbf{C}^\Delta(s)\right]\mathbf{S}_r(s), \quad (11)$$

that is equivalent to:

$$\begin{aligned} &\mathbf{S}^0(s) - \mathbf{S}_r(s) = \mathbf{T}_r(s) - \mathbf{T}^0(s) = \\ &= \mathbf{T}^0(s)\left(\mathbf{C}^0(s)\right)^{-1}\mathbf{C}^\Delta(s)\mathbf{S}_r(s). \end{aligned} \quad (12)$$

Solving for $\mathbf{C}^\Delta(s)$ leads to (7).

Equation (7) can be used to compute the frequency response of the controller increments by taking the frequency response over a suitable frequency range $[\omega_1, \omega_N]$.

To retuning the parameters of the PID controller, the frequency response of $\mathbf{C}^\Delta(j\omega)$ is approximated by $\mathbf{C}_{PID}^\Delta(j\omega)$, which has the following form:

$$\mathbf{C}_{PID}^\Delta(j\omega) = \mathbf{K_P}^\Delta + \frac{\mathbf{K_I}^\Delta}{j\omega} + \mathbf{K_D}^\Delta j\omega, \quad (13)$$

where $\mathbf{K_P}^\Delta$, $\mathbf{K_I}^\Delta$ and $\mathbf{K_D}^\Delta \in R^{n\times n}$ are the PID controller increments.

Then, the following convex optimization problem can be written to obtain the increments:

$$\begin{aligned} \min_{\mathbf{K_P}^\Delta, \mathbf{K_I}^\Delta, \mathbf{K_D}^\Delta} \quad & \left\| \begin{bmatrix} \Re\left(\mathbf{C}^\Delta(j\omega)\right) \\ \Im\left(\mathbf{C}^\Delta(j\omega)\right) \end{bmatrix} - \begin{bmatrix} \Re\left(\mathbf{C}_{PID}^\Delta(j\omega)\right) \\ \Im\left(\mathbf{C}_{PID}^\Delta(j\omega)\right) \end{bmatrix} \right\|_2^2 \\ & \forall \omega \in [\omega_1, \omega_N], \\ \text{s.t.} \quad & \mathbf{K_P}^\Delta, \mathbf{K_I}^\Delta, \mathbf{K_D}^\Delta \text{ are diagonal,} \end{aligned} \quad (14)$$

where $\Re(.)$ and $\Im(.)$ are the real and imaginary parts, respectively. The final controller is then obtained by (6).

An issue in this formulations is that there are no stability constraints. That said, the resulting closed-loop may be

unstable. This problem will be solved by adding further constraints on the optimization problem.

3.2 Stability constraints

In order to guarantee stability and robustness of the IMC redesign procedure, constraints will be added to problem in (14).

To keep the problem convex and of simple implementation, the procedure presented in Euzébio et al. (2020) was adopted. It consists in divide the MIMO system in a set of SISO subsystems, represented by effective transfer functions to account for loop interactions. Then, the linear margin constraints approach proposed in Karimi et al. (2007) can be applied to each subsystem, in order to guarantee stability and robustness margins of each individual loop.

By denoting $G_j^{ef}(s)$ as the ETF of jth loop. It is defined as the transfer function between jth input and jth output, by keeping this loop open while the remaining are closed. A procedure to calculate the ETF is presented in Silva and Barros (2020).

The effective loop transfer function (ELTF) is defined as:

$$L_j^{ef}(s) = G_j^{ef}(s)C_j(s). \tag{15}$$

Considering $C_j(s) = C_j^0(s) + C_j^{\Delta}(s)$ in PID form, as shown in (3) and (13), then the ELTF can be written as:

$$L_j^{ef}(s) = \rho_j^T G_j^{ef}(s)\phi_j(s), \tag{16}$$

where:

$$\begin{aligned} \rho_j &= \left[k_{p_j}^0 + k_{P_j}^{\Delta},\ k_{I_j}^0 + k_{I_j}^{\Delta},\ k_{D_j}^0 + k_{D_j}^{\Delta}\right]^T, \\ \phi_j(s) &= \left[1,\ \frac{1}{s},\ \frac{s}{T_{fj}s+1}\right]^T. \end{aligned} \tag{17}$$

The Nyquist plot of $L_j^{ef}(j\omega)$ is presented in Fig. 2. It should lie in the right side of the line r_n, which crosses the negative real axis between 0 and -1 at a distance l from the critical point. The angle of slope is α, which varies between 0° and 90°.

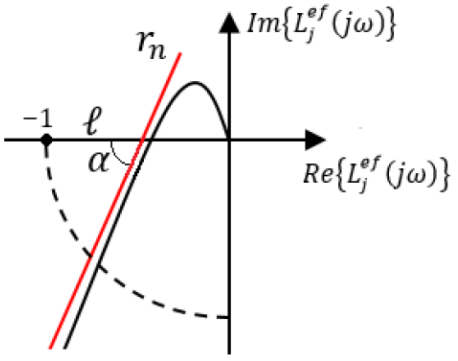

Fig. 2. Nyquist plot of ELTF and linear constraints (Silva and Barros, 2020).

With the line parameters l and α, the following lower bounds can be obtained for the gain, phase and modulus margins of the ETF, respectively:

$$\begin{aligned} g_m &\geq \frac{1}{1-l}, \\ \phi_m &\geq \arccos\left((1-l)\sin^2\alpha + \cos\alpha\sqrt{1-(1-l)^2\sin^2\alpha}\right), \\ M_m &\geq l\sin\alpha. \end{aligned} \tag{18}$$

By geometric analysis, the constraints are met if, and only if:

$$\rho_j^T\left(\cot\alpha\Im_j^{ef}(j\omega) - \Re_j^{ef}(j\omega)\right) + l \leq 1, \tag{19}$$

where $\Im_j^{ef}(j\omega)$ and $\Re_j^{ef}(j\omega)$ are, respectively, the imaginary and real parts of $G_j^{ef}(j\omega)\phi_j(j\omega)$.

3.3 Resulting optimization problem with constraints

By combining the unconstrained optimization problem in (14) and the linear constraints in (19), the resulting problem can be written as (21).

In some cases, in order to achieve the specification, some of the gains can have a change in sign, implying that the direction of the control action is different than that of the loop direction. This may cause issues in the controller implementation because the reset or rate time will be negative. To avoid this, a restriction is added to guarantee that the direction of control action is kept during optimization:

$$d_j\rho_j^T \geq [0\ 0\ 0]\ \ \forall\ j, \tag{20}$$

where $d_j = 1$ if the control action of jth loop is direct, and $d_j = -1$ if it is reverse.

$$\begin{aligned} \min_{\mathbf{K_P}^{\Delta},\mathbf{K_I}^{\Delta},\mathbf{K_D}^{\Delta}} \quad & \left\| \begin{bmatrix} \Re\left(\mathbf{C}^{\Delta}(j\omega)\right) \\ \Im\left(\mathbf{C}^{\Delta}(j\omega)\right) \end{bmatrix} - \begin{bmatrix} \Re\left(\mathbf{C}_{PID}^{\Delta}(j\omega)\right) \\ \Im\left(\mathbf{C}_{PID}^{\Delta}(j\omega)\right) \end{bmatrix} \right\|_2^2 \\ & \forall\omega \in [\omega_1, \omega_N], \\ \text{s.t.} \quad & \rho_j^T\left(\cot\alpha\Im_j^{ef}(j\omega) - \Re_j^{ef}(j\omega)\right) + l \leq 1 \\ & \qquad \forall\ j,\ \forall\ \omega \in [\omega_1, \omega_N], \\ & d_j\rho_j^T \geq [0\ 0\ 0]\ \ \forall\ j, \\ & \mathbf{K_P}^{\Delta}, \mathbf{K_I}^{\Delta}, \mathbf{K_D}^{\Delta} \text{ are diagonal.} \end{aligned} \tag{21}$$

The main advantages of (21) is that it is convex and can be easily implemented in solvers such as MATLAB *fmincon* or CVX.

4. SIMULATION RESULTS

In this section, the proposed method is applied to two MIMO processes: the Wood and Berry (1973) distillation column and the reactor of a diesel hydrotreating unit (Aguiar et al., 2023).

The centralized IMC PID retuning method of Aguiar et al. (2021) and the decentralized IMC PID tuning method of Jeng and Lee (2023) are used as comparison. In the first scenario, the objective was to verify the efficacy of the decentralized structure against the centralized. In the second scenario, the objective was to compare with other method of decentralized IMC PID design in frequency domain.

In order to achieve a fast closed-loop response, the reference model time constants were chosen as $\tau_j = (T_{jj} +$

$L_{jj})/3$, where T_{jj} and L_{jj} are the dominant time constant and delay of $G_{jj}(s)$, respectively. In both examples, the linear margins were set as $l = 0.67$ and $\alpha = 60°$, which results in $M_S < 1.7$ for each loop.

The choice of the frequency ranges was made by considering the maximum critical frequency among the elements of the reference model $\mathbf{T_r}(s)$, ω_c. Then, N log spaced points were taken as $\omega_k = k\omega_c/N$, where $k = 1, \cdots, N$.

To assess the control system performance relative to the desired reference ($\mathbf{T_r}(s)$), the adopted criterion was the integral squared error between the output ($y_j(t)$) and the output of reference model ($y_{r_j}(t)$):

$$E_j = \sum_{\infty}^{t=1} (y_j(t) - y_{r_j}(t))^2. \tag{22}$$

Also, to measure the control effort, the total variation (TV) of the manipulated variables is considered. It is defined as:

$$TV_j = \sum_{\infty}^{t=1} |u_j(t+1) - u_j(t)|. \tag{23}$$

To analyze the stability and robustness of the closed-loop system, the nyquist diagrams of the ELTFs are showed. The aim is to compare the retuned controller with the initial controller, and see if the frequency margin constraints are met.

4.1 Example 1

Consider the Wood and Berry (1973) model for the binary distillation column:

$$\mathbf{G}(s) = \begin{bmatrix} \frac{12.8e^{-s}}{16.7s+1} & \frac{-18.9e^{-3s}}{21s+1} \\ \frac{6.6e^{-7s}}{10.9s+1} & \frac{-19.4e^{-3s}}{14.4s+1} \end{bmatrix}, \tag{24}$$

with the following reference model:

$$\mathbf{T}_r(s) = \begin{bmatrix} \frac{e^{-1s}}{5.9s+1} & 0 \\ 0 & \frac{e^{-3s}}{5.8s+1} \end{bmatrix}. \tag{25}$$

The initial controller is:

$$\mathbf{C}^0(s) = \begin{bmatrix} 0.5 + \frac{0.1}{s} & 0 \\ 0 & -0.1 - \frac{0.01}{s} \end{bmatrix}. \tag{26}$$

Controllers $\mathbf{C}(s)$, $\mathbf{C}^1(s)$ and $\mathbf{C}^2(s)$ were obtained using proposed, Jeng and Lee (2023) and Aguiar et al. (2021) methods, respectively. The transfer matrices of each one are:

$$\mathbf{C}(s) = \begin{bmatrix} 0.206 + \frac{0.023}{s} + 0.003s & 0 \\ 0 & -0.1 - \frac{0.012}{s} - 0.002s \end{bmatrix}, \tag{27}$$

$$\mathbf{C}^1(s) = \begin{bmatrix} 0.152 + \frac{0.023}{s} + 0.003s & 0 \\ 0 & -0.078 - \frac{0.012}{s} - 0.002s \end{bmatrix}, \tag{28}$$

$$\mathbf{C}^2(s) = \begin{bmatrix} 0.206 + \frac{0.022}{s} + 0.003s & -0.025 - \frac{0.017}{s} + 0.001s \\ 0.206 + \frac{0.008}{s} - 0.002s & -0.101 - \frac{0.012}{s} - 0.002s \end{bmatrix}. \tag{29}$$

Two closed-loop experiment were performed to compare the performance between designs. An unit step is applied to the setpoint each loop at different times, in order to observe the effects of setpoint tracking and coupling between loops. In Fig. 3, it is shown the comparison between the proposed and Jeng and Lee (2023) method, while in Fig. 4 is presented the comparison between the decentralized and centralized methods. For both cases, the desired reference response of $\mathbf{T}_r$ is plotted, as well as the response with the initial controller. The error indexes between the outputs and reference outputs, calculated using (22), and the total variation of the MVs, calculated using (23), are shown in Table 1.

In comparison with the (Jeng and Lee, 2023) IMC design, it is possible to note that the retuned controller leads to a better closed-loop performance, with a lower error between the reference response. When compared with the retuned centralized controlled, the performance was worse, specially in respect to the decoupling obtained with each controller. This effect was expected because of the simpler structure of the proposed controller and the high coupling between the loops.

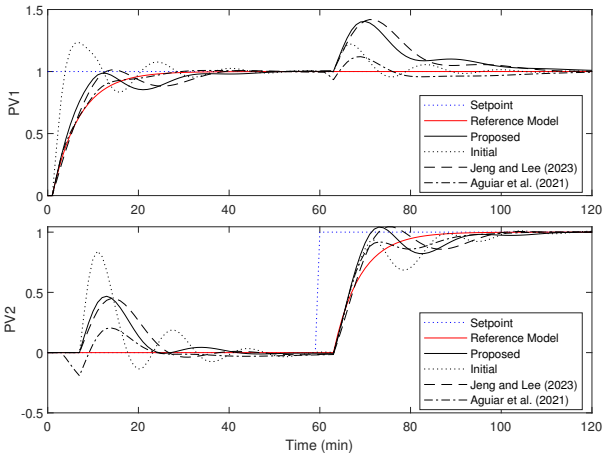

Fig. 3. closed-loop step response of example 1 with comparison between the centralized and decentralized methods.

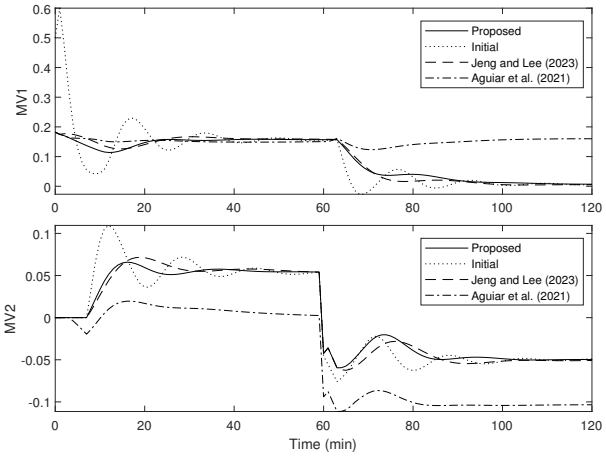

Fig. 4. manipulated variables of the closed-loop step response of example 1.

To assess the robustness of the controller designed with proposed method, the Nyquist diagrams of the ELTFs of each loop were plotted. They are shown in Fig.

Table 1. Error indexes and TVs for example 1.

	E_1	E_2	TV_1	TV_2
Proposed	1.79	2.04	0.27	0.29
Initial	2.99	4.09	1.46	0.52
Jeng and Lee (2023)	2.02	2.10	0.27	0.28
Aguiar et al. (2021)	0.13	0.52	0.13	0.24

Fig:nyquistwb, in comparison with the initial ELTFs and the line constraint. For both loops, the poor stability margins with initial controller were improved by redesign, and the restrictions were met.

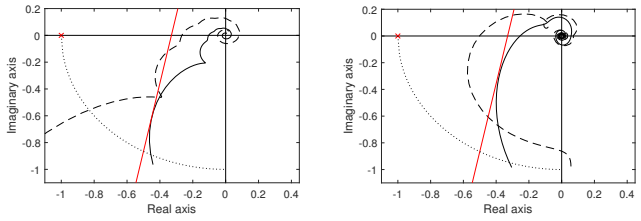

(a) Loop 1 (b) Loop 2

Fig. 5. Nyquist diagrams of ELTFs with proposed (solid line) and initial controller (dashed line) for example 1, in comparison with line constraint (red line).

4.2 Exemple 2

Consider a diesel hydrotreating unit (HDT). The process model, reference closed-loop model and designed controllers are all presented in Equation (30).

Similar to example 1, $\mathbf{C}^{(0)}(s)$ is the initial controller, $\mathbf{C}(s)$ the redesigned decentralized controller, $\mathbf{C}^{(1)}(s)$ was obtained by applying Jeng and Lee (2023) method, and $\mathbf{C}^{(2)}(s)$ is the retuned centralized controller that was obtained by applying Aguiar et al. (2021) method.

Because of the lower triangular structure of $\mathbf{G}(s)$, the centralized PID controller $\mathbf{C}^{(2)}(s)$ also is triangular.

The closed-loops step responses are presented in Figs. 6 and 7, to compare both decentralized methods and the redesigns decentralized and centralized methods, respectively. The error indexes between the outputs and reference outputs are shown in Table 2. The total variation of each MV is presented in Table 3.

In this example, because of the lower coupling between loops, the decentralized redesign method leads to good results for both setpoint tracking and decoupling. In comparison with the centralized controller, it leads to a better closed-loop performance for loops 1 and 3, even with a simpler structure.

Table 2. Error indexes for example 2.

	Loop 1	Loop 2	Loop 3	Loop 4
Proposed	4.53	26.10	23.15	40.91
Initial	63.06	109.60	82.11	138.55
Jeng and Lee (2023)	6.35	36.44	33.01	46.69
Aguiar et al. (2021)	7.22	9.05	71.12	37.21

In Fig. 8, the Nyquist diagrams of each ELTF are presented. With the redesigned controller, it was possible to achieve a faster closed-loop response than initial controller without violate the margin constraints.

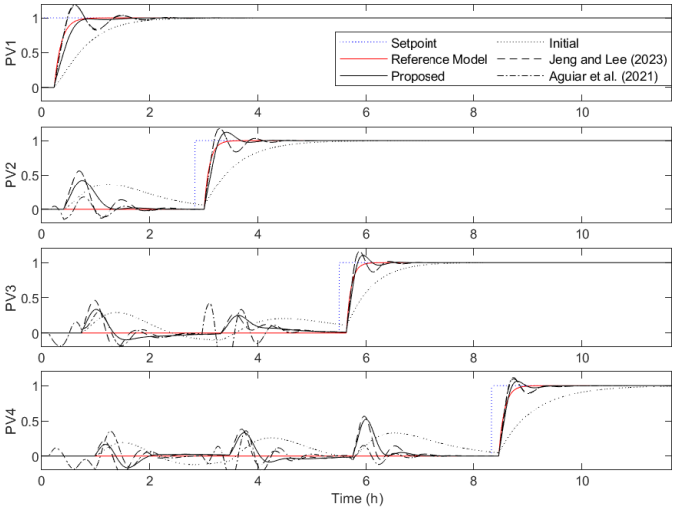

Fig. 6. closed-loop step response of example 2 with comparison between the centralized and decentralized methods.

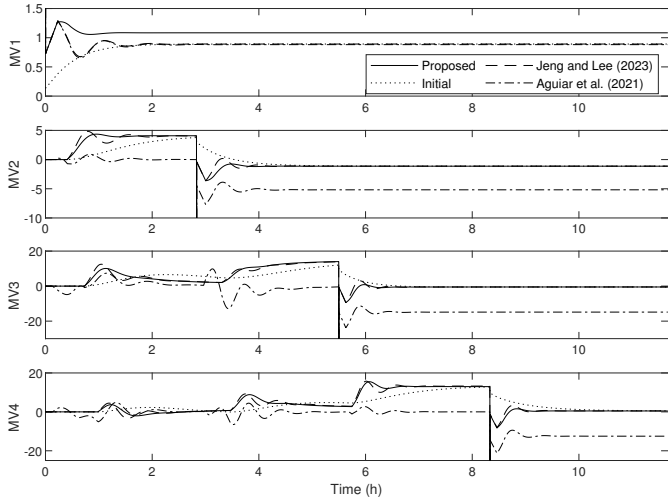

Fig. 7. manipulated variables of the closed-loop step response of example 2.

Table 3. TVs for example 2.

	Loop 1	Loop 2	Loop 3	Loop 4
Proposed	8.8	153.7	654.4	592.8
Initial	0.8	8.7	28.4	30.2
Jeng and Lee (2023)	9.6	160.7	672.6	617.0
Aguiar et al. (2021)	9.7	156.9	720.3	639.4

5. CONCLUSION

A procedure for retuning decentralized controllers was proposed. It consists in solve a convex optimization problem to approximate the frequency response of the new controller with a PID structure, in order to achieve the closed-loop specification. To guarantee stability and robustness, linear margin constraints are applied to shape the effective loop transfer functions. The method was validate through simulations, where good performance indexes were achieved when compared with other decentralized and a centralized controller, while keeping the stability constraints.

$$\mathbf{G}(s) = \begin{bmatrix} \frac{1.1215e^{-838s}}{538.01s+1} & 0 & 0 & 0 \\ \frac{0.8785e^{-1478s}}{882.82s+1} & \frac{-0.1931e^{-612.78s}}{433.16s+1} & 0 & 0 \\ \frac{0.8770e^{-2646.46s}}{878.77s+1} & \frac{-0.1647e^{-1699.31s}}{2378.17s+1} & \frac{-0.0674e^{-473.21s}}{455.03s+1} & 0 \\ \frac{0.9321e^{-3568s}}{1052.2s+1} & \frac{-0.1588e^{-2299.74s}}{1363.77s+1} & \frac{-0.0572e^{-882.65s}}{949.36s+1} & \frac{-0.0783e^{-475.87s}}{693.15s+1} \end{bmatrix}, \quad \mathbf{T}_r(s) = \begin{bmatrix} \frac{e^{-838s}}{473.7s+1} \\ \frac{e^{-613s}}{348.6s+1} \\ \frac{e^{-473s}}{309.4s+1} \\ \frac{e^{-476s}}{389.7s+1} \end{bmatrix}$$

$$\mathbf{C}^{(0)}(s) = \text{diag}\begin{bmatrix} 0.134 + \frac{0.0003}{s} \\ -0.829 - \frac{0.002}{s} \\ -2.898 - \frac{0.006}{s} \\ -3.146 - \frac{0.005}{s} \end{bmatrix}, \quad \mathbf{C}(s) = \text{diag}\begin{bmatrix} 0.43 + \frac{0.0006}{s} + 14.75s \\ -2.80 - \frac{0.005}{s} - 7.52s \\ -11.02 - \frac{0.019}{s} - 56.13s \\ -11.65 - \frac{0.015}{s} - 122.42s \end{bmatrix}, \quad \mathbf{C}^{(1)}(s) = \text{diag}\begin{bmatrix} 0.72 + \frac{0.0007}{s} + 0.80s \\ -4.41 - \frac{0.005}{s} - 6.88s \\ -14.60 - \frac{0.019}{s} - 29.44s \\ -14.38 - \frac{0.015}{s} - 25.81s \end{bmatrix}, \tag{30}$$

$$\mathbf{C}^{(2)}(s) = \begin{bmatrix} 0.73 + \frac{0.0007}{s} + 0.86s & 0 & 0 & 0 \\ -0.96 + \frac{0.003}{s} + 3.83s & -4.41 - \frac{0.005}{s} - 6.89s & 0 & 0 \\ 3.21 + \frac{0.001}{s} + 15.44s & -13.67 - \frac{0.013}{s} + 17.59s & -14.56 - \frac{0.019}{s} - 29.38s & 0 \\ -3.33 + \frac{0.0009}{s} + 3.81s & 0.73 + \frac{0.0007}{s} + 0.86s & -1.16 + \frac{0.014}{s} + 4.09s & -14.87 - \frac{0.015}{s} - 28.36s \end{bmatrix}.$$

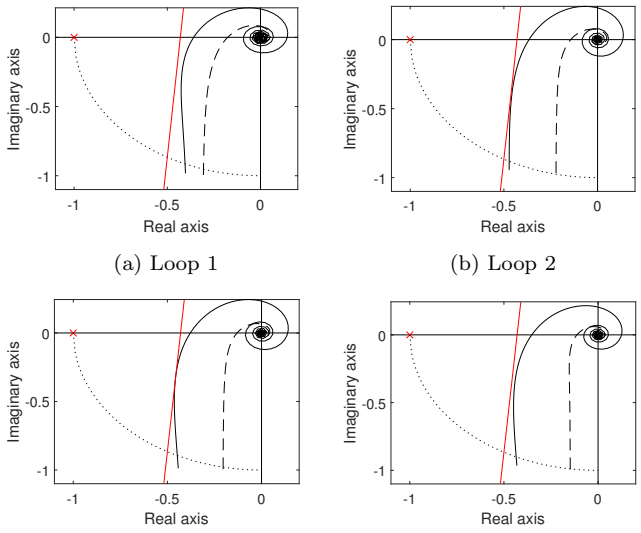

(a) Loop 1 (b) Loop 2

(c) Loop 3 (d) Loop 4

Fig. 8. Nyquist diagrams of ELTFs with proposed (solid line) and initial controller (dashed line) for example 2, in comparison with line constraint (red line).

For future works, the constraints on the optimization problem may be improved by taking into account multivariable stability specifications.

REFERENCES

Aguiar, A.P.V.A., Júnior, G.A., Barros, P.R., and Perkusich, A. (2021). A closed-loop frequency domain pi retuning technique for multivariable systems. *IFAC-PapersOnLine*, 54(3), 463–468. doi: 10.1016/j.ifacol.2021.08.285. 16th IFAC Symposium on Advanced Control of Chemical Processes ADCHEM 2021.

Aguiar, A.P.V.d.A., Longhi, L.G.S., Acioli Júnior, G., Zani, A., and Barros, P.R. (2023). Inverted decoupling pid control applied to the reactors of a diesel hydrotreating unit. *Journal of Control, Automation and Electrical Systems*, 34(2), 315–323. doi:10.1007/s40313-022-00977-0.

Euzébio, T.A., Yamashita, A.S., Pinto, T.V., and Barros, P.R. (2020). Siso approaches for linear programming based methods for tuning decentralized pid controllers. *Journal of Process Control*, 94, 75–96. doi: 10.1016/j.jprocont.2020.08.004.

Gao, X., Yang, F., Shang, C., and Huang, D. (2017). A novel data-driven method for simultaneous performance assessment and retuning of pid controllers. *Industrial & Engineering Chemistry Research*, 56(8), 2127–2139. doi: 10.1021/acs.iecr.6b03893.

Garrido, J., Ruz, M.L., Morilla, F., and Vázquez, F. (2022). Iterative design of centralized pid controllers based on equivalent loop transfer functions and linear programming. *IEEE Access*, 10, 1440–1450. doi: 10.1109/ACCESS.2021.3139214.

Jeng, J.C. and Lee, M.W. (2023). Multi-loop pid controllers design with reduced loop interactions based on a frequency-domain direct synthesis method. *Journal of the Franklin Institute*, 360(4), 2476–2506. doi: 10.1016/j.jfranklin.2023.01.002.

Karimi, A., Kunze, M., and Longchamp, R. (2007). Robust controller design by linear programming with application to a double-axis positioning system. *Control Engineering Practice*, 15(2), 197–208. doi: 10.1016/j.conengprac.2006.06.002.

Nisi, K., Nagaraj, B., and Agalya, A. (2019). Tuning of a pid controller using evolutionary multi objective optimization methodologies and application to the pulp and paper industry. *International Journal of Machine Learning and Cybernetics*, 10(8), 2015–2025. doi: 10.1007/s13042-018-0831-8.

Silva, M.T. and Barros, P.R. (2020). An iterative procedure for tuning decentralized pid controllers based on effective open-loop process. In *2020 7th International Conference on Control, Decision and Information Technologies (CoDIT)*, volume 1, 813–818. doi: 10.1109/CoDIT49905.2020.9263823.

Silva Moreira, L.J., Aguiar, A.P.V.A., Barros, P.R., and Acioli Júnior, G. (2021). Data-driven pid closed-loop evaluation and retuning time and frequency domain approaches. *Journal of Control, Automation and Electrical Systems*, 32(1), 82–95. doi:10.1007/s40313-020-00654-0.

Wood, R. and Berry, M. (1973). Terminal composition control of a binary distillation column. *Chemical Engineering Science*, 28(9), 1707–1717. doi:10.1016/0009-2509(73)80025-9.